

# Poly(2-Methoxyethyl Acrylate) (PMEA)-Coated Anti-Platelet Adhesive Surfaces to Mimic Native Blood Vessels through HUVECs Attachment, Migration, and Monolayer Formation

Haque, Md Azizul

Murakami, Daiki

Anada, Takahisa

Tanaka, Masaru

<https://hdl.handle.net/2324/7161729>

---

出版情報 : Coatings. 12 (6), pp.869-, 2022-06-20. MDPI AG  
バージョン :  
権利関係 : Creative Commons Attribution 4.0 International



## Article

# Poly(2-Methoxyethyl Acrylate) (PMEA)-Coated Anti-Platelet Adhesive Surfaces to Mimic Native Blood Vessels through HUVECs Attachment, Migration, and Monolayer Formation

Md Azizul Haque <sup>1,2</sup> , Daiki Murakami <sup>1,3,\*</sup> , Takahisa Anada <sup>1,3</sup>  and Masaru Tanaka <sup>1,3,\*</sup> 

<sup>1</sup> Department of Chemistry and Biochemistry, Graduate School of Engineering, Kyushu University, Fukuoka 819-0395, Japan; md.azizul.haque.509@s.kyushu-u.ac.jp (M.A.H.); takahisa\_anada@ms.infoc.kyushu-u.ac.jp (T.A.)

<sup>2</sup> Department of Applied Chemistry and Chemical Engineering, Noakhali Science and Technology University, Noakhali 3814, Bangladesh

<sup>3</sup> Institute for Materials Chemistry and Engineering, Kyushu University, Fukuoka 819-0395, Japan

\* Correspondence: daiki\_murakami@ms.infoc.kyushu-u.ac.jp (D.M.); masaru\_tanaka@ms.infoc.kyushu-u.ac.jp (M.T.); Tel./Fax: +81-92-802-6238 (D.M. & M.T.)

**Abstract:** Confluent monolayers of human umbilical vein endothelial cells (HUVECs) on a poly(2-methoxyethyl acrylate) (PMEA) antithrombogenic surface play a major role in mimicking the inner surface of native blood vessels. In this study, we extensively investigated the behavior of cell–polymer and cell–cell interactions by measuring adhesion strength using single-cell force spectroscopy. In addition, the attachment and migration of HUVECs on PMEA-analogous substrates were detected, and the migration rate was estimated. Moreover, the bilateral migration of HUVECs between two adjacent surfaces was observed. Furthermore, the outer surface of HUVEC was examined using frequency-modulation atomic force microscopy (FM-AFM). Hydration was found to be an indication of a healthy glycocalyx layer. The results were compared with the hydration states of individual PMEA-analogous polymers to understand the adhesion mechanism between the cells and substrates in the interface region. HUVECs could attach and spread on the PMEA surface with stronger adhesion strength than self-adhesion strength, and migration occurred over the surface of analogue polymers. We confirmed that platelets could not adhere to HUVEC monolayers cultured on the PMEA surface. FM-AFM images revealed a hydration layer on the HUVEC surfaces, indicating the presence of components of the glycocalyx layer in the presence of intermediate water. Our findings show that PMEA can mimic original blood vessels through an antithrombogenic HUVEC monolayer and is thus suitable for the construction of artificial small-diameter blood vessels.

**Keywords:** poly(2-methoxyethyl acrylate) (PMEA); human umbilical vein endothelial cell (HUVEC); cell–cell interaction; cell adhesion strength; cell migration; frequency-modulation atomic force microscopy (FM-AFM); hydration; artificial small-diameter blood vessel



**Citation:** Haque, M.A.; Murakami, D.; Anada, T.; Tanaka, M. Poly(2-Methoxyethyl Acrylate) (PMEA)-Coated Anti-Platelet Adhesive Surfaces to Mimic Native Blood Vessels through HUVECs Attachment, Migration, and Monolayer Formation. *Coatings* **2022**, *12*, 869. <https://doi.org/10.3390/coatings12060869>

Academic Editor: Michelina Catauro

Received: 21 May 2022

Accepted: 17 June 2022

Published: 20 June 2022

**Publisher's Note:** MDPI stays neutral with regard to jurisdictional claims in published maps and institutional affiliations.



**Copyright:** © 2022 by the authors. Licensee MDPI, Basel, Switzerland. This article is an open access article distributed under the terms and conditions of the Creative Commons Attribution (CC BY) license (<https://creativecommons.org/licenses/by/4.0/>).

## 1. Introduction

According to the World Health Organization (WHO), due to the rapid increase in cardiovascular diseases (CVDs) and the associated number of deaths, the 17.9 million deaths from CVDs in 2019 is estimated to increase to 23.6 million by 2030 [1,2]. Approximately 32% of total deaths worldwide are caused by the diverse categories of CVDs, such as coronary heart disease (CHD) and peripheral artery disease (PAD). Currently, researchers are focusing on obtaining the most suitable treatments for CVDs. To date, angioplasty, atherectomy, stent insertion, and bypass of the injured vessels are the most well-known treatments [3]. Bypass of injured vessels is an effective treatment, and autologous saphenous vessels are generally selected. However, there is a risk of secondary trauma. Therefore, synthetic artificial vascular grafts can be suitable alternatives to autologous saphenous

vessels. To date, polyethylene terephthalate (PET) and expanded polytetrafluoroethylene (ePTFE) have been used as synthetic grafts for large-diameter vessels. However, these grafts show poor patency for small-diameter blood vessels due to thrombus formation inside them [4]. PET and ePTFE are unable to promote endothelialization and induce thrombosis and inflammation due to platelet and neutrophil activation [5]. Therefore, vascular graft diameter smaller than 6 mm presents a high risk of thrombus formation. In addition, protein adsorption boosts the platelet adhesion in surface induced clotting [6].

Many methods have been implemented to improve the surface of synthetic grafts through surface modification, new polymer development, and cell–substrate interaction investigation using mechanobiology assessments. Various surface modification techniques have been used to functionalize the substrate interface for cell attachment, growth, migration, rapid endothelialization, and long-term anticoagulation [7–9]. Polymer coating is an effective approach to functionalize biomaterial surfaces. Functionalization with poly(ethylene glycol) and zwitterionic polymers, including poly(2-methacryloyloxyethyl phosphorylcholine) (PMPC), suppresses biofilm formation, immune responses to biomaterial surfaces, and adhesion of platelets [10–16]. Moreover, several approaches have been introduced to obtain smart or responsive surfaces. Temperature-responsive grafted polymer brushes based on LCST open opportunities for the fabrication of responsive surfaces [17]. On the other hand, stimuli-responsive macromolecules have significantly impacted new developments in polymeric coatings where the surface shows responsiveness to bacterial attacks, ice or fog formation, anti-fouling properties, autonomous self-cleaning and self-healing, or drug delivery systems [18].

A stable, confluent endothelium lining may act as a completely antithrombogenic surface. However, such an endothelial cell (EC) layer does not form spontaneously at the surface of a vascular implant in humans *in vivo*. Subsequently, one researcher has proposed pre-seeding ECs or progenitor cells prior to implantation in order to increase the patency of synthetic vascular grafts [19,20]. However, poor cell adhesion ability under flow condition indicates low compatibility [21]. Consequently, polymers with antifouling and antithrombogenic properties with strong endothelial cell attachment abilities are desirable for researchers to develop artificial small-diameter blood vessels (ASDBVs) that can mimic native blood vessels.

In this regard, poly(2-methoxyethyl acrylate) (PMEA), an antithrombogenic synthetic polymer, is a suitable alternative to ePTFE and PET because of its intermediate water (IW, loosely bound water) content, which is a measure of biocompatibility and blood compatibility [22,23]. It was found that IW is present in natural biocompatible polymers, such as DNA (and RNA), heparin, and chondroitin sulfate [24]. PMEA is a US Food and Drug Administration (FDA)-approved biocompatible polymer used in artificial lungs, catheters, and stents as an antithrombogenic coating material. PMEA is water insoluble and hydrophobic in nature. It makes thin film coatings on substrates, such as PET or other surfaces where coating needs to be performed. When the biomaterials contact with the body fluids, the primary interaction happens on the biomaterial–fluid interface in hydrated state. First, proteins are adsorbed and then denatured on the hydrated material surface. Cell adherent protein adsorption depends on the wettability, polymer rich and poor regions, as well as the microphase separation of a homopolymer at an interface. The amount and degree of denaturation of adsorbed proteins affect subsequent cell behavior, including cell adhesion, migration, proliferation, and differentiation. The modification in the chemical structure of PMEA shows distinct morphological and interaction behavior with the blood component [25,26]. A polymer with similar chemical and structural properties to PMEA is named PMEA analogous polymer. Our recent investigation reveals that PMEA analogous polymers suppress platelet adhesion, and the degree of suppression depends on the amount of IW present in each polymer [22,26]. In particular, a polymer with high IW content (e.g., PMPC, IW = 11.11% w) suppresses platelets more effectively than a polymer with low IW content [27]. However, PMPC does not allow the attachment of cells, proteins, or any other blood components on its surface.

A monolayer of ECs can effectively protect surfaces from the adhesion of blood components (platelets, white blood cells, red blood cells, and proteins), thus suppressing platelet coagulation and thrombus formation [28]. Alternatively, PMEA, a blood-compatible polymer, does not activate leukocytes, erythrocytes, or platelets, *in vitro* [22]. Furthermore, because PMEA and analogous polymers promote the attachment of non-blood cells, they are believed to facilitate endothelialization [29]. Therefore, endothelialization over the polymer surface may play a major role in surface antithrombogenic properties.

In recent years, the human umbilical vein endothelial cells (HUVEC) model has been used in cardiovascular and clinical research as compared to animal models. *In vitro* HUVEC models have been convenient to study platelet adhesion to the endothelium, endothelial dysfunctions, the potential effect of atherosclerosis in initial stages and atherosclerosis progression [30,31]. On the other hand, EC activation, migration, and proliferation are responsible for the formation and organization of tubular structures to form new blood vessels through the angiogenesis process [32,33]. Finally, HUVEC as a model to study the endothelium has greatly facilitated the study of cardiovascular disease. In contrast, the glycocalyx is a combination of hydrated sugar-rich molecules (heparin sulfate, chondroitin sulfate, and hyaluronic acid) coating the surface of ECs lining the inside of blood vessels. Our previous study showed that promoting the glycocalyx of HUVECs with transforming growth factor- $\beta$ 1 (TGF- $\beta$ 1) decreased platelet adhesion, while degrading the glycocalyx with heparinase I increased platelet adhesion. These results suggested that the glycocalyx of cultured HUVECs modulates platelet compatibility, and the amount of glycocalyx secreted by HUVECs depends on the chemical structure and cross-linker concentration of the scaffolds [34]. Matrix stiffness is also known to affect the expression of the glycocalyx in cultured ECs [35].

In the present study, we aim to find the best polymer from PMEA analogous polymers that can be used to construct an artificial small diameter vascular graft as a coating material. For this purpose, the polymer should fulfil the basic needs, such as antithrombogenic surface, good HUVECs attachment, growth, proliferation, migration, monolayer formation, and strong adhesion strength to the surface. We used HUVECs to measure cell–cell and cell–substrate interactions using single-cell force spectroscopy (SCFS). We found a possible mechanism of HUVECs monolayer formation over a biocompatible polymer surface by comparing the strength of cell–cell and cell–substrate interactions. We then evaluated the migration behavior of HUVECs on the PMEA polymer analogs. In addition, the bilateral migration of HUVECs between two adjacent polymer surfaces was observed, indicating migration of HUVECs from native blood vessels to artificial implants *in vitro*. Furthermore, a platelet adhesion test was performed on HUVECs monolayers cultured on PMEA and PET. Finally, the upper surface of a single HUVEC was investigated using frequency-modulation atomic force microscopy (FM-AFM) to determine the hydration states of the HUVEC surface to verify the expression of the glycocalyx layer as well as IW states.

## 2. Materials and Methods

### 2.1. Chemicals and Materials

Hydrophilized PET sheet (thickness = 120  $\mu$ m) was purchased from Mitsubishi Plastic Inc. (Tokyo, Japan). PMEA ( $M_n$  = 26.9 kg/mol,  $M_w/M_n$  = 2.73), poly(3-methoxypropyl acrylate) (PMC3A,  $M_n$  = 20.8 kg/mol,  $M_w/M_n$  = 3.83), and poly(*n*-butyl acrylate) (PBA,  $M_n$  = 62.8 kg/mol,  $M_w/M_n$  = 1.41) were synthesized as previously reported [26]. Poly(*n*-butyl methacrylate-co-2-methacryloyloxyethyl phosphorylcholine) (BMA 70 mol%, MPC 30 mol%) (PMPC,  $M_w$  = 600 kg/mol) was a gift from the NOF Corporation, Tokyo, Japan. Tissue culture polystyrene (TCPS) was purchased from IWATA, Japan. The chemical structures of the polymers used in the present study are shown in Figure 1. Fibronectin was purchased from Wako Pure Chemical Industries (Osaka, Japan). The platelet adhesion test was performed using human whole blood, which was purchased from Tennessee Blood Services (Memphis, TN, USA). Human whole blood was collected from healthy donors and stored in a vacuum blood collection tube (Venoject II; Terumo Co., Tokyo, Japan) containing 3.2% sodium

citrate as an anticoagulant. Blood was used within a week after collection. Blocking reagent was purchased from Nacalai Tesque (Kyoto, Japan). All other reagents and solvents were obtained from Kanto Chemical Co. (Tokyo, Japan).

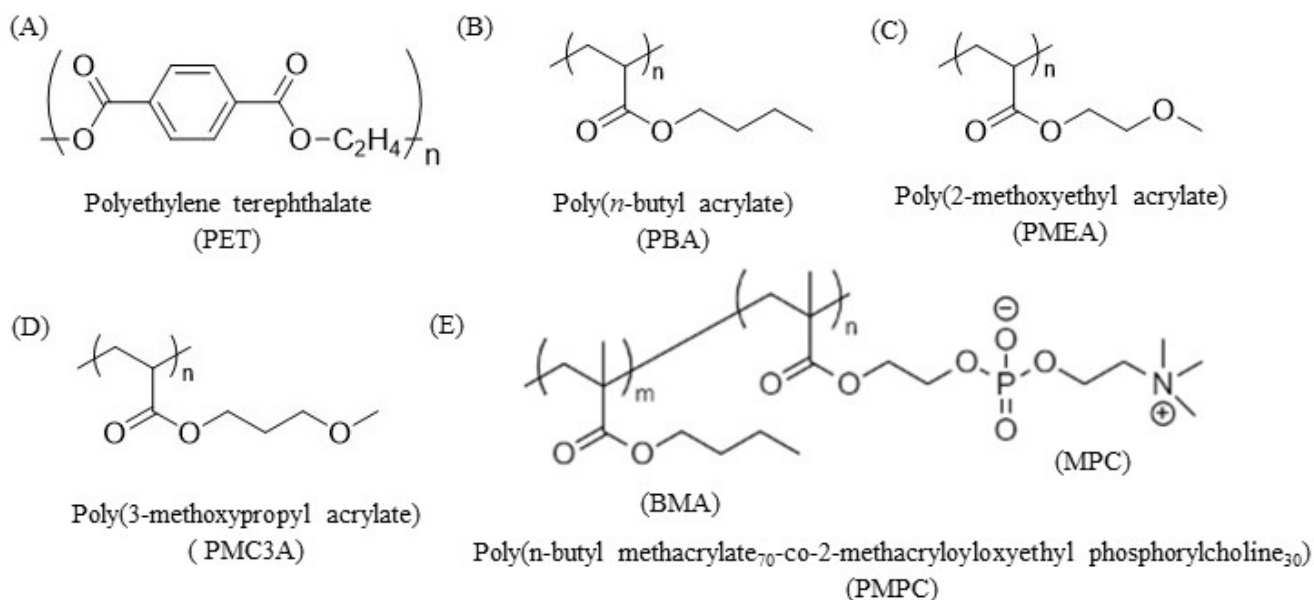


**Figure 1.** Chemical structure of (A) polyethylene terephthalate (PET); (B) poly(*n*-butyl acrylate) (PBA); (C) poly(2-methoxyethyl acrylate) (PMEA); (D) poly(3-methoxypropyl acrylate) (PMC3A), and (E) poly(*n*-butyl methacrylate-co-2-methacryloyloxyethyl phosphorylcholine) (BMA 70 mol%, MPC 30 mol%) (PMPC).

## 2.2. Fabrication of Polymer-Coated Substrates

PET was used as a substrate for the polymer coating. Initially, the PET sheet was cut into a circular shape with a diameter of 14 mm using a hand press cutter and cleaned by washing with toluene. PMEA, PMC3A, and PBA were dissolved in toluene (0.5% *w/v*) to obtain the polymer solution. PMPC was dissolved in methanol at the same concentration. The PMEA analogous polymer solutions of 40  $\mu$ L were charged on the PET substrates for spin-coating using a Spin Coater (Mikasa MS-A100) at a constant speed of 3000 rpm for 40 s, ramped down for 4 s, and then dried for at least for 24 h in a vacuum dryer at 25  $^{\circ}$ C. Bare PET was used as the positive control and TCPS was used as the cell culture dish. The morphologies of the polymer-coated surfaces were observed by atomic force microscopy (AFM) and the thickness was estimated at around 100 nm using transmission electron microscopy [25,36]. The surface roughness of all polymer coatings was almost the same within 10–20 nm. However, AFM observation showed that the interfacial structures of the PMEA and PMC3A were highly ordered, homogeneous, and compactly dispersed in nanometer scale, although the low blood-compatible polymer PBA interface had an irregular structure [25].

## 2.3. Contact Angle

Contact angle measurements were conducted using milli Q water. Two methods (sessile drop and air bubble) were used to measure the contact angle values of PMEA analogous surfaces at 25  $^{\circ}$ C using a DropMaster DMO-501SA (Kyowa Interface Science Co., Tokyo, Japan) (shown in Table 1). Following the sessile drop method, 2  $\mu$ L of water droplet was dropped on the polymer surface for 60 s, and the contact angles were calculated from the photograph. In the captive bubble method, PMEA analogous substrates were immersed in Milli-Q water for 24 h. Then, a 2  $\mu$ L air bubble was injected beneath the substrate surfaces located in water, and the contact angles were also measured using photographic images. Finally, the contact angle at 30 s was counted as the contact angle of that substrate.

**Table 1.** Contact angle and water content of studied polymers.

Polymers	Contact Angle * [deg]			
	Sessile Water Drops	Captive Air Bubble		IW
	(30 s)	(30 s)	24 h	(wt.%)
PET	73.3 ( $\pm 0.9$ )	125.5 ( $\pm 2.2$ )	125.4 ( $\pm 0.5$ )	0
PBA	83.8 ( $\pm 1.9$ )	126.7 ( $\pm 2.8$ )	125.0 ( $\pm 1.7$ )	0.31
PMEA	44.3 ( $\pm 2.1$ )	134.0 ( $\pm 0.9$ )	132.9 ( $\pm 1.8$ )	3.7
PMC3A	52.1 ( $\pm 0.5$ )	126.9 ( $\pm 1.0$ )	127.8 ( $\pm 0.7$ )	2.8
PMPC	108.9 ( $\pm 0.5$ )	152.4 ( $\pm 2.9$ )	150.0 ( $\pm 3.8$ )	11.11

\* 2  $\mu$ L water droplet in air (sessile drop) and 2  $\mu$ L air bubble in water (Captive bubble). The data represent the means  $\pm$  SD (n = 5).

#### 2.4. HUVECs Culture

ECs were solely used for all experiments described in this article. Commercially available HUVECs (Lonza, Cologne, Germany) were cultured under static cell culture conditions (37 °C, 5% CO<sub>2</sub>) in polystyrene-based cell culture flasks. Cells were used for 4–6 passages and cultured in endothelial basal medium (EBM-2) supplemented with endothelial growth medium (EGM-2) Single Quots<sup>®</sup> kit and 2% fetal calf serum (FCS; Lonza). Before starting the experiments, cells were detached using 0.25% trypsin/EDTA solution (Thermo Fisher Scientific, Rockford, IL, USA) from the culture dish. Then, HUVECs solution was centrifugated for 3 min at 1200 rpm to isolate HUVECs from the medium. Initial cell counting was performed using a hemocytometer to adjust the cell density.

#### 2.5. Cell Attachment, Proliferation, and Immunocytochemical Analysis

Cell attachment and proliferation assays were performed using a 24-well plate (IWATA). The 24-well plate was first coated with PMPC (0.5% *w/v*) and allowed to dry. The pre-coated polymer substrates were then fixed onto the 24-well plate using glue on the back side of each substrate and cured under UV light for 30 min. Phosphate-buffered saline (PBS) was then added to the wells and incubated for 1 h at 37 °C. Afterwards, culture media were added and incubated for another hour at 37 °C. HUVECs were seeded on the substrates at  $1 \times 10^4$  cells/cm<sup>2</sup> in serum-containing media and allowed to adhere and proliferate on the surface of the substrates for 1 h, 1 day, or 3 days. After cultivation at these specific time intervals, the cells were analyzed using ImageJ software (version 1.53C; National Institutes of Health, Bethesda, MD, USA).

In addition, before starting the immunocytochemical analysis, the prepared substrates were preconditioned, as in the cell attachment and proliferation assays. HUVECs were seeded ( $5 \times 10^3$  cells/cm<sup>2</sup>) on polymer-coated PET substrates and incubated for 1, 24, or 72 h. After culturing for specific times, the cells were fixed using preheated (37 °C) 4% (*w/v*) paraformaldehyde (Fujifilm Wako Pure Chemical Co., Ltd., Osaka, Japan) and stored outside for 10 min. Thereafter, 1% (*v/v*) Triton X-100 (Fujifilm Wako Pure Chemicals Co., Ltd.) in PBS (–) was added to increase plasma membrane permeability. After washing, the sections were blocked for 30 min. Then, the substrates were stained with mouse monoclonal anti-human vinculin antibody (VIN-11-5; Sigma-Aldrich, St. Louis, MO, USA) (1:200) diluted in PBS (–) for 90 min at room temperature (RT), and subsequently stained with Alexa Fluor 568-conjugated anti-mouse immunoglobulin G (IgG) (H + L) antibody (1:1000 dilution), Alexa Fluor 488-conjugated phalloidin (1:1000 diluted), and 4,6-diamidino-2-phenylindole (DAPI, 1:1000 dilution) (all from Thermo Fisher Scientific, Waltham, MA, USA), all diluted in 10% blocking solution in PBS, treated for 1 h at RT. After performing these steps, stained cells were fixed on glass slides. Fluorescence photographs were taken using a confocal laser-scanning microscope (CLSM) (FV-3000; Olympus, Tokyo, Japan). The HUVEC morphology was quantitatively assessed using ImageJ.

## 2.6. HUVECs Migration Analysis

HUVECs migration analyses were executed in six-well plates. Initially, one half of the PET substrate ( $\varphi = 30$  mm) was coated with a PMEA-analogous polymer and the other half was exposed to bare PET. First, HUVECs were cultured on all studied substrates, placed into six-well plates with a seeding density  $1 \times 10^4$  cells/cm<sup>2</sup> and incubated at 37 °C until full confluency. After confluency, the cell monolayer surface was scratched using a 4 mm wide rubber cell scraper in the PET–polymer interface region and kept in incubator for migration. Finally, cell migration towards the scratched area was observed at 0, 24, and 48 h of scratching, and time-lapse images were taken using a phase-contrast microscope (Figure 2). The migrated area was quantified using ImageJ software and denoted as  $A_0 - A_t$ , where  $A_0$  is the initial area before migration and  $A_t$  is the area at the certain time  $t$  (i.e., 0, 24, or 48 h). The migration rate was then plotted against the types of substrates where migration happened.

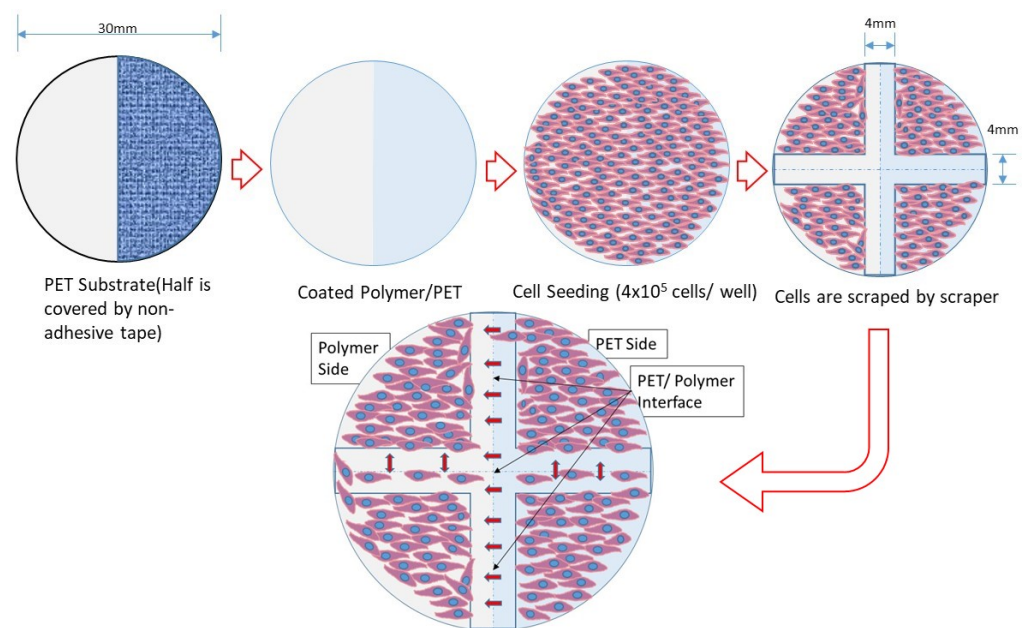


**Figure 2.** Schematic representation of the HUVECs migration rate measurements and observation of HUVECs migration through the coated polymer-PET interface.

## 2.7. HUVEC-PMEA and HUVEC-HUVEC Interaction Determined by SCFS

Prior to the HUVEC–PMEA interaction measurement, the PMEA-coated substrates were placed under UV light for 30 min before the PBS was poured and placed in incubator for 1 h at 37 °C. Subsequently, EGM-2 medium was added to the substrate and freshly detached cells (five to six passages) were injected into it. In addition, the tipless cantilever named TL-CONT (spring constant  $k = 0.2$  N/m; Bruker, Billerica, MA, USA) was coated with fibronectin solution (1 mg/mL) and kept for around 20 min to dry. Then, a single HUVEC was captured with a tipless cantilever for 10 min with set point: 2 nN. The force–distance curves between the cells and the substrates were measured using an AFM (CellHesion JPK; Bruker, Billerica, MA, USA) equipped with a tipless cantilever (set point: 2 nN, approaching rate: 5.0  $\mu$ m/s, holding time: 120 s, retraction rate: 15  $\mu$ m/s). The value of set point for the measurement of HUVEC adhesion strength was used from our previous report, where the relationship between the set points and the cell adhesion strength of HeLa cells were evaluated [37]. In this investigation, the maximum force for cell detachment from the substrate is denoted as adhesion force, which is indicated at the lowest point of the retraction curve. Adhesion work was estimated as the amount of work required to detach the cell from the substrate, corresponding to the area enclosed by the baseline and retraction curve [38]. The same experimental conditions were used to determine HUVEC–HUVEC interactions. The only exception was that HUVECs were cultured on both the

PMEA-coated PET substrate and TCPS. HUVEC adhesion strength was measured on the attached HUVECs using the same procedure as described earlier in this section.

### 2.8. Platelet Adhesion Test on Cultured HUVECs Monolayer

The platelet adhesion test was performed under static conditions as previously described [22,34,39]. In brief, fresh blood was centrifuged at  $400\times g$  for 5 min to obtain platelet-rich plasma (PRP), and the remaining blood was centrifuged at  $2500\times g$  for 10 min to obtain platelet-poor plasma (PPP). The platelet concentration was determined using a hemocytometer. Cell density ( $4 \times 10^7$  cells/cm<sup>2</sup>) was adjusted by mixing PPP and PRP. Prior to this experiment, HUVECs were cultured on the PMEA-coated and bare PET substrates. Before loading the platelet suspension, the cultured HUVECs layer was washed with PBS (–). Then, 450 µL of platelet suspension was loaded onto HUVECs proliferated on the confluent layer and incubated for 1 h at 37 °C. After 1 h of incubation, the weakly adhered platelets were rinsed three times with PBS. Adhered platelets were then fixed using 1% glutaraldehyde for 2 h at 37 °C. After this period, samples were rinsed with PBS, 50% PBS, and Milli-Q water. Finally, the samples were dried at RT for 1–2 days before being subjected to sputter gold coating for scanning electron microscopy (SEM) observation. Then, the number of adhered platelets was counted from SEM images using ImageJ software ( $n = 15$  of each substrate).

### 2.9. FM-AFM of Single HUVEC Surface

FM-AFM was conducted using an SPM-8100FM (Shimadzu Co., Kyoto, Japan) in water at 23 °C. A PPP-NCHAuD cantilever (typical spring constant,  $k = 42$  N/m, NanoWorld AG, Neuchâtel, Switzerland) was used. The resonance frequency in water was approximately 140 kHz, and the scan in the z-direction was performed with a force limit of 2.5 V, which corresponds to a frequency shift of approximately 500 Hz. The amplitude of the cantilever oscillation was maintained constant at approximately 2 nm.

### 2.10. Statistical Analyses

Data from at least three independent trials were used in calculation of mean  $\pm$  standard deviation (SD). Significant differences were assessed using one-way analysis of variance (ANOVA) (Tukey–Kramer multiple comparison test) with Origin Pro (version 2019b; OriginLab Co., Northampton, MA, USA).  $p < 0.05$  was set to evaluate statistical significance.

## 3. Results and Discussion

### 3.1. HUVECs Cultured on PMEA-Analogous Polymers

The formation of confluent EC monolayers on implanted materials has been identified as a method to avoid thrombus formation [28,40]. PMEA polymer analogs (PMEA, PMC3A, and PBA) and PMPC were coated on PET substrates to culture HUVECs and investigate HUVECs adhesion ability. The physical properties of the studied polymer are shown in Table 1. HUVECs attachment ability depends on the surface type, morphology, and biomechanical interaction in the interface. In our previous study, we mentioned the surface morphology of our polymer studied by AFM observation [25]. Figure 3 shows the phase-contrast micrographs of the sub-confluent to confluent layer of HUVECs attached to the PMEA polymers at 120 h. Bare PET and PMPC were used as the positive and negative controls, respectively. It was found that HUVECs can attach to PMEA polymer analogs and form a confluent monolayer. This confirms our previous findings that ECs can attach, proliferate, and form a layer on PMEA-coated surfaces compared with other analogous polymers. The proliferation of HUVECs on the various substrates decreased in the following order: TCPS > PET  $\approx$  PMEA > PMC3A  $\approx$  PBA > PMPC. No considerable number of HUVECs was found on PMPC at 120 h. HUVECs could not survive on PMPC because of their strong antithrombogenic properties. These results agree with those of our previous study in which HUVECs and aorta smooth muscle cells (AoSMCs) were cultured on PET, PMEA, and PMPC [41].

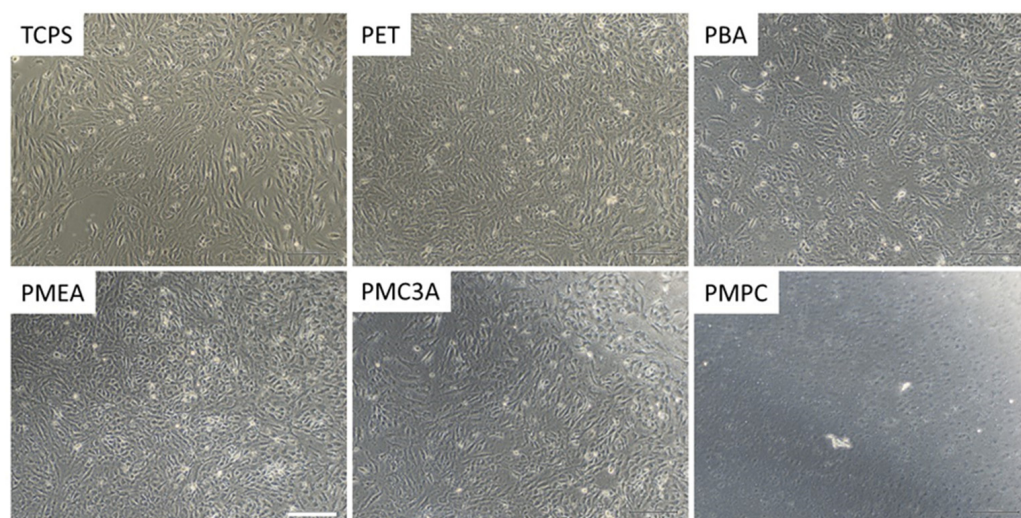


**Figure 3.** Phase-contrast micrographs of the HUVECs cultured for 120 h on PMEA-analogous polymers and on TCPS, PET, and PMPC as controls (scale bar = 200  $\mu$ m).

The different attachment behaviors of HUVECs on PMEA-analogous polymers depend on the hydration state, surface morphology, and stiffness of each polymer [35,40,42]. Generally, cells adhere to a polymeric surface via cell-binding proteins, such as fibronectin or fibrinogen, through integrin [43]. HUVECs are more likely to adhere to fibronectin than fibrinogen through the RGD sequence, which is a universal binding site [44]. It has been proven that cells can attach to PMEA in an integrin-dependent and -independent manner through direct interaction between the cell membrane and the polymer interface [45]. In this study, we found a more confluent HUVECs monolayer on PMEA-coated substrates than on other analogous polymers. This can be attributed to the selective protein adsorption and integrin-independent and -dependent adhesion mechanism of PMEA, which is regulated by the IW content [41].

### 3.2. Possible Mechanism of HUVECs Monolayer Formation on PMEA (Cell-Cell Interaction)

The initial interactions between individual HUVECs cultured on the PMEA surface were measured using the SCFS. Figure 4 shows the HUVEC adhesion strength in nN, measured at three different places of the attached HUVEC on PMEA. We found that the adhesion strength was highest in the external cellular matrix (ECM) of the attached single HUVEC, lower on arbitrary positions of the monolayer, and lowest on the top of the cell where the nucleus is present. Therefore, variation in interaction strength can occur because of the concentration of adhesion proteins in the serum medium. Previous studies have shown that cell adhesion on PMEA in serum-free medium is similar to that on serum-containing medium [45]. In contrast, the adhesion energy differed among the various interaction locations of the attached HUVEC, which may be due to the dissimilar surface interaction area and number of focal adhesion points.

In contrast, intercellular adhesion plays a major role in tissue development and homeostasis [46]. Sancho et al. measured the cell adhesion forces of HUVECs on substrates in well-attached individual cells and monolayers. In the present study, we measured and compared the initial HUVEC adhesion strength between HUVEC–PMEA and HUVEC–HUVEC, where the HUVECs were cultured on both TCPS and PMEA surfaces, as shown in Figure 5. The average HUVEC–HUVEC interaction strength was calculated, as shown in Figure 4, and results revealed that there is no effect of culture substrates on cell–cell interaction strength. However, the HUVEC–PMEA adhesion strength was much higher than the cell–cell interaction. Therefore, initially, HUVECs seem to be more involved in attachment to the substrates than individual cells, even though a few portions of seeded cells were in a tri-dimensional (3D) aggregated form. After seeding, the cells spread and formed a two-dimensional (2D) layer. Therefore, the initial cell adhesion strength is a measure of

monolayer formation. This result shows that the measurement of cell adhesion strength is vital for the development of endothelial monolayers for the construction of ASDBV. In addition, ECs forming the inner wall of every blood vessel are constantly exposed to the mechanical forces generated by blood flow [47]. If the cell–substrate interaction is not sufficient to resist the force exerted by blood flow, then no cell can be attached or migrate to form a confluent layer of cells. Therefore, EC responses to these hemodynamic forces and interaction strength play a critical role in the homeostasis of the circulatory system in the development of ASDBV.

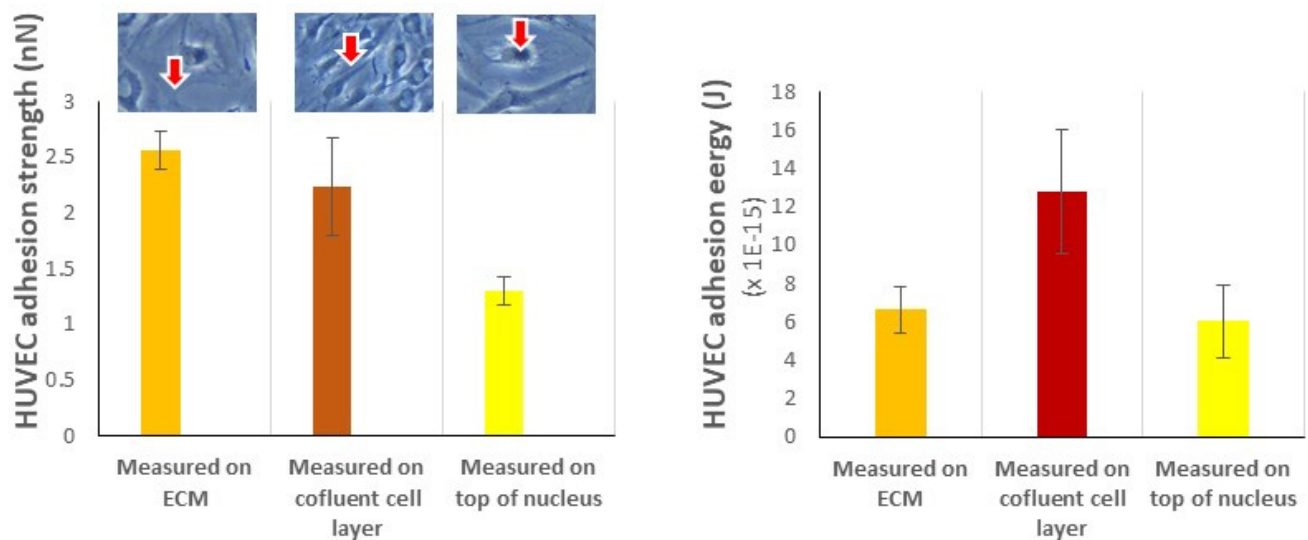


**Figure 4.** Cell-cell interaction strength measured in three positions (ECM, arbitrary point of confluent layer, top of nucleus) of confluent HUVECs monolayer. The data represent the mean  $\pm$  SD ( $n = 4$ ). Red arrows represent the typical positions at which the force measurements were done.

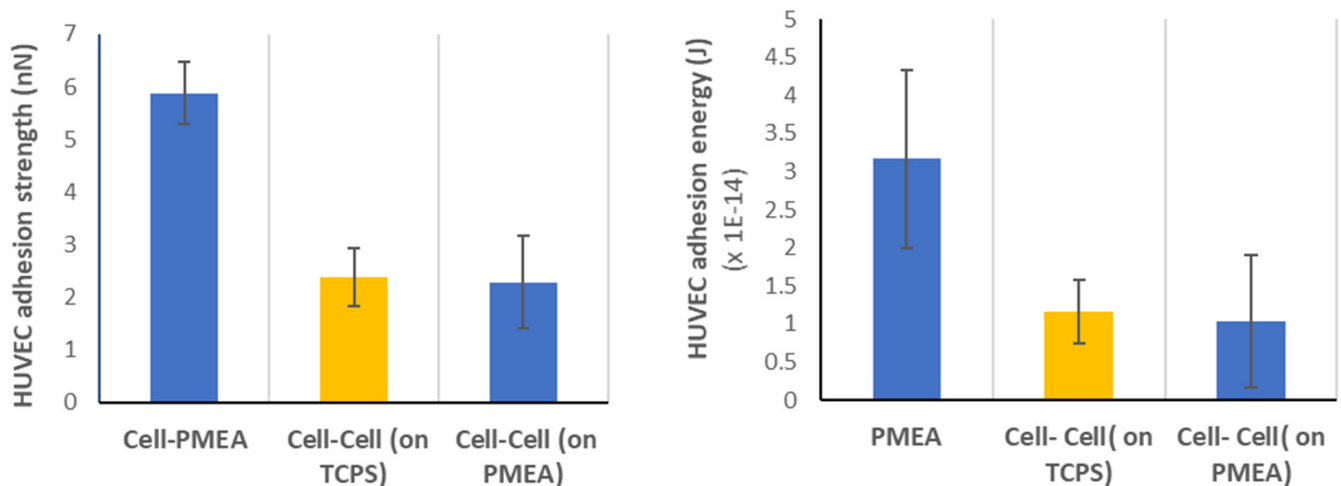


**Figure 5.** Comparison of HUVEC adhesion strength between cell-PMEA, cell-cell cultured on TCPS, and cell-cell cultured on PMEA. The data represent the mean  $\pm$  SD ( $n > 4$ ).

### 3.3. HUVECs Migration Analysis

HUVECs migration analysis was performed to evaluate the migration ability of HUVECs on the different polymeric surfaces. Figure 6 shows the HUVECs migration analysis on the PMEA, PMC3A, PBA, and PET. The left side of each substrate was coated on the polymer side, and the right side was always bare PET. The white dotted line in each image indicates the interface between the PMEA-analogous and bare PET. The migration time was recorded from 0 to 48 h using a time-lapse microscope. The red dotted line indicates

the area occupied by HUVECs before and after migration at the various time intervals. In Figure 2, we demonstrate the HUVECs migration procedure, in which the layer of HUVECs was scratched in both the vertical and horizontal directions. After migration, five locations were selected for each substrate to calculate the migration rate. From Figure 6, we can see that those cultured monolayers of HUVECs were scratched using a rubber scraper to set the initial area of cultured HUVECs on PMEAnalogous polymer and PET surfaces. Then, images were taken every hour for 48 h.

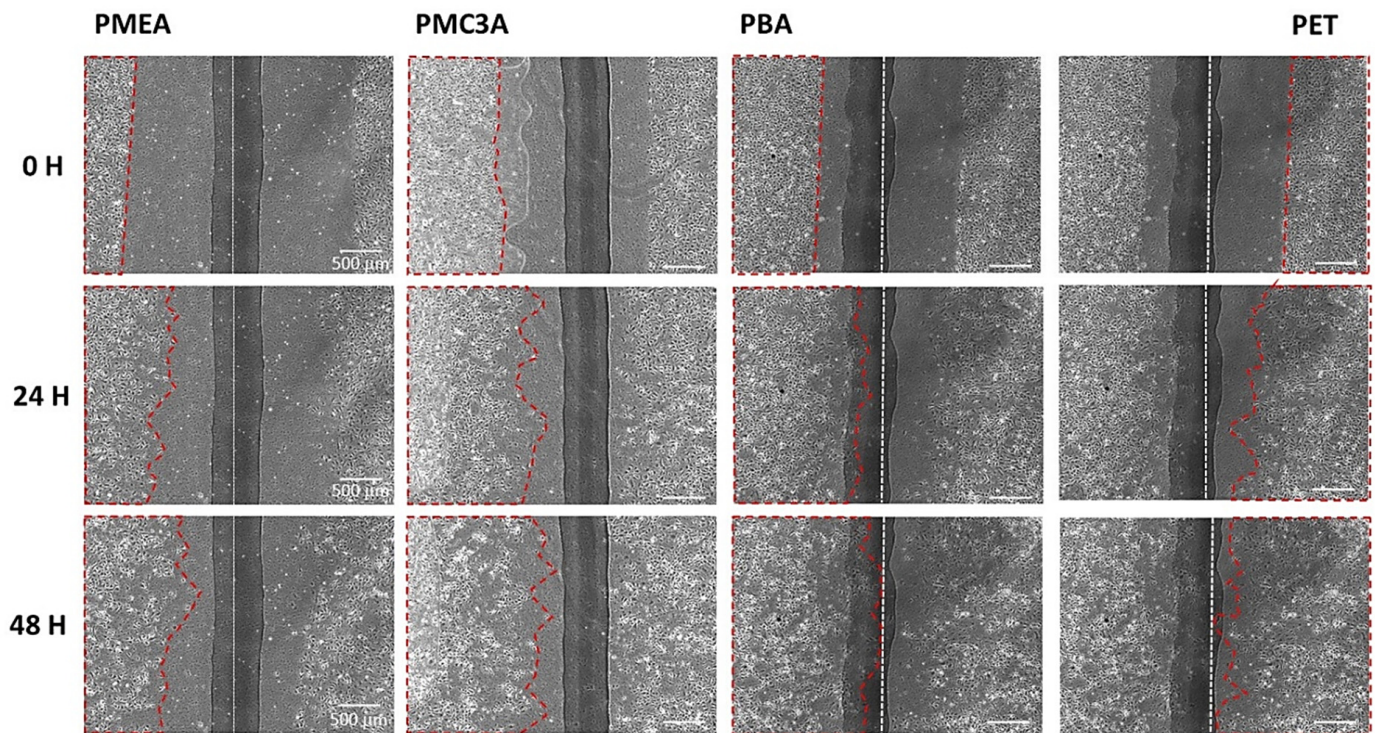


**Figure 6.** HUVECs migration analysis on PMEAnalogous, PMC3A, PBA, and PET (scale bar = 500  $\mu\text{m}$ ). The white dotted line indicates the interface between PMEAnalogous polymers and bare PET. Migration was recorded from 0 to 48 h. The red dotted line indicates the HUVECs occupied area before and after migration.

### 3.4. Observation of Cell Migration between Surfaces

In addition, we observed HUVECs migration between the surfaces through the interface. Focusing on the interface (white dotted line) of each polymer, we identified the migration of HUVECs from the bare PET side to the PMEAnalogous side through the interface. The migration is marked by a red rectangle in Figure 7, and it increased with time. Furthermore, we calculated the HUVECS migration rate for all the substrates from the newly covered area after migration. We found that the migration rates were slightly different, although the differences were not statistically significant (Figure 8). However, PMEAnalogous showed the highest average migration rate among all samples.

The most vital task of ECs is to protect the vascular system through the formation of an antithrombogenic monolayer that is periodically renewed to maintain proper endothelial functions [48,49]. To treat CVDs, after the implementation of cardiovascular devices or artificial blood vessels, the capacity to migrate ECs toward injured or foreign surfaces is crucial. Endothelization and migration of HUVECs are influenced by many factors, including the physical and chemical properties of polymers, surface characteristics, and adhesion of binding proteins on specific polymeric substrates. In the present study, PMEAnalogous showed similar migration behavior, although PMEAnalogous polymers have dissimilar wet abilities, surface characteristics, and binding protein adsorption abilities, as already known from our previous study. These effects did not affect the migration rate

of HUVECs. In addition, migration from the bare PET to the PMEA side confirmed the mimetic behavior of native blood vessels.

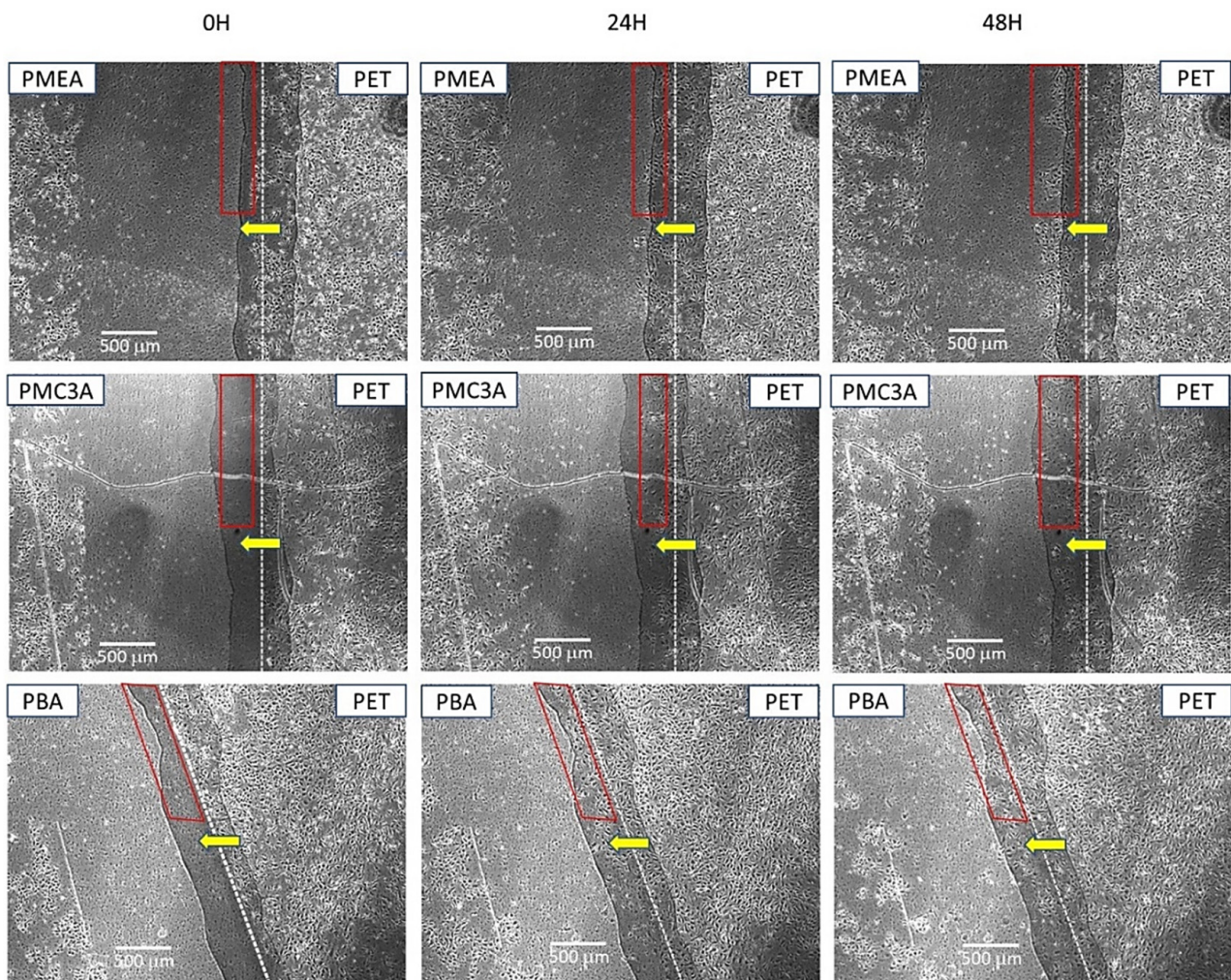


**Figure 7.** Observation of HUVECs migration between the substrate surfaces (scale bar = 500  $\mu\text{m}$ ). Time laps imaging confirmed the HUVECs migration from PET to polymers through the interface of PMEA-PET, PMC3A-PET, and PBA-PET. Migration was recorded from 0 to 48 h. The migration processes are marked with red rectangles and yellow arrows.

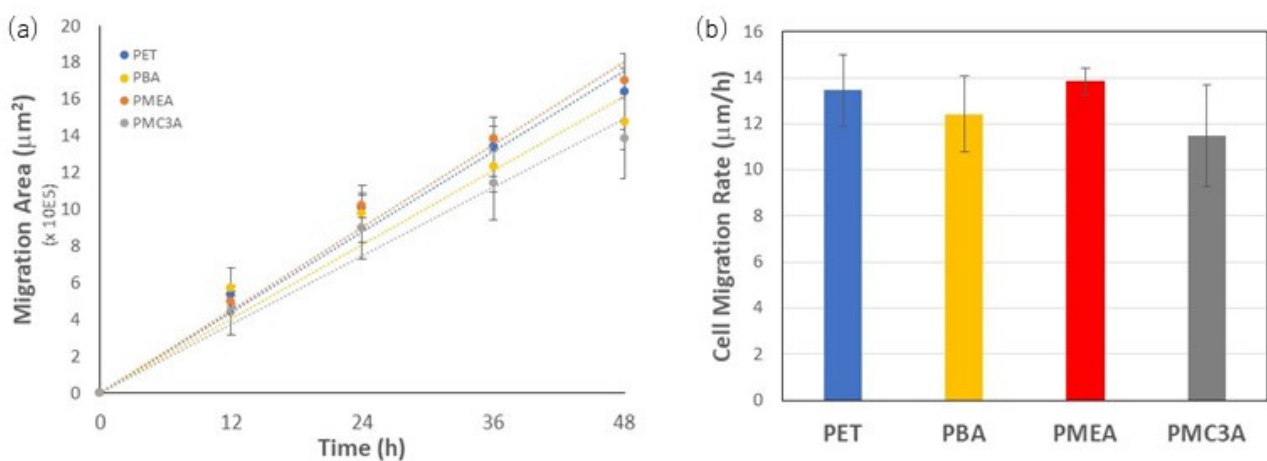


**Figure 8.** (a) Migration area (b) migration rate on PMEA-analogous polymers and bare PET. The data represent the mean  $\pm$  SD ( $n = 5$ ).  $p < 0.05$  was used to define statistical significance.

### 3.5. Platelet Adhesion on HUVECs Monolayer Cultured on Polymers Film

The biocompatibility and antithrombogenic behavior of PMEAs-analogous polymers have already been studied based on different factors, such as contact angle, protein adsorption, surface roughness, polymer chain length, platelet adhesion behavior, and IW content of each polymer. In the present study, we limited our investigation to only PMEAs and PET because of the results of previous platelet adhesion tests under static conditions. PMEAs showed an antithrombogenic surface compared with PET, where more platelets were adhered. In contrast, there is no significant study on platelet adhesion on a HUVECs monolayer that acts as an internal antithrombogenic surface of real blood vessels.

Figure 9 shows confocal images from the immunocytochemical analysis of HUVECs cultured on PMEAs and PET. These CLSM images reveal that a similar type of HUVECs monolayer was formed on PET and PMEAs. In addition, the shape of adhered HUVECs was comparable in both substrates. In our previous study, we found that cell adhesion depends on the integrin-mediated binding protein adhesion to the specific surface, known as integrin-dependent adhesion [45]. However, cells can adhere to PMEAs through direct physicochemical contact (integrin-independent contact) and via integrin-dependent adhesion. Furthermore, the HUVEC adhesion strength on PMEAs was similar to that on PET. If the PET-based artificial vascular graft needs to be replaced because of thrombus formation after implementation, PMEAs seem to offer the best alternative due to its proven antithrombogenicity. We observed that the number of platelets was much higher on bare PET (Figure 10a) than bare PMEAs (Figure 10e), which agrees with our previous studies [23,41,50]. In contrast, few adhered platelets were found on the HUVECs monolayer on PET (Figure 10b–d), and this was lower than in the bare PET. However, no significant number of platelets was found on the surfaces of HUVECs cultured on PMEAs (Figure 10f–h). Therefore, PMEAs seem to keep its antithrombogenic activity before and after HUVECs monolayer formation on PMEAs. A summary of the platelet adhesion test is shown in Figure 10i. This antithrombogenic property of HUVECs monolayer on PMEAs is essential to the construction of ASDBV. Further investigations are still needed regarding blood flow conditions, including in vivo experiments, for additional confirmation of this antithrombogenic property of PMEAs.

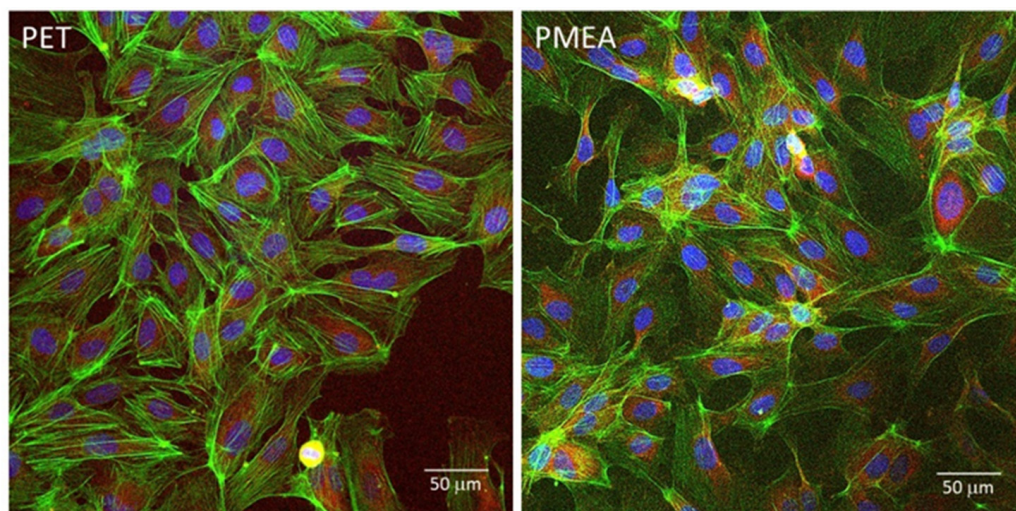


**Figure 9.** CLSM images of HUVECs cultured on PET and PMEA-coated surface. Blue: Cell nuclei; green: vinculin; red: actin fiber.

### 3.6. FM-AFM of HUVECs Surface

To investigate the antithrombogenic activity of the HUVEC monolayer on PMEAs from the hydration state perspective, FM-AFM was performed. Figure 11 shows the results of the FM-AFM ( $z$ - $x$  scan) on the HUVEC–PBS interface. The repulsive layer observed is marked in blue and white, demonstrating the degree of frequency shift. This repulsive layer may be attributed to the glycocalyx, which is composed of a hydrated sugar-rich layer. Our

previous work demonstrated that such a hydrated polymer layer could contribute to the antithrombogenicity of the surfaces [51]. The repulsive layer on HUVEC was thicker than 10 nm. This is thicker than that observed on the PMEA spin-coated surface (approximately 5 nm) and thinner than that on the PMPC spin-coated surface (approximately 20 nm) on PET (see Figure S1 in Supplementary Material). Thus, the FM-AFM results corroborated the high antithrombogenic activity of the HUVEC monolayer on PMEA, as well as the platelet adhesion test results.

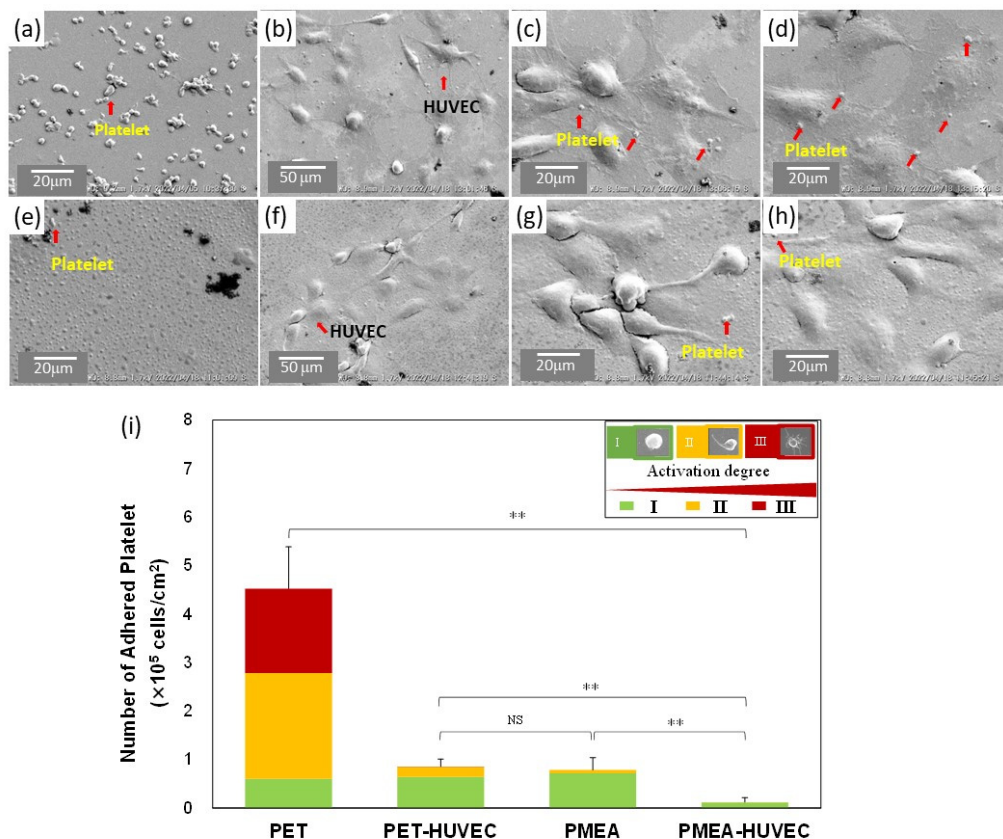


**Figure 10.** SEM image of (a) bare PET; (b) HUVEC monolayer on PET (scale bar = 50 μm); (c,d) HUVEC monolayer on PET (scale bar = 20 μm); (e) bare PMEA; (f) HUVEC monolayer on PMEA (scale bar = 50 μm); and (g) and (h) HUVEC monolayer on PMEA (scale bar = 20 μm). Red arrows indicate the typical positions of observed cells. (i) Number of adhered platelets counted from SEM images. The data represent the means ± SD, n = 15, \*\*  $p < 0.05$ ; NS means not significant difference).

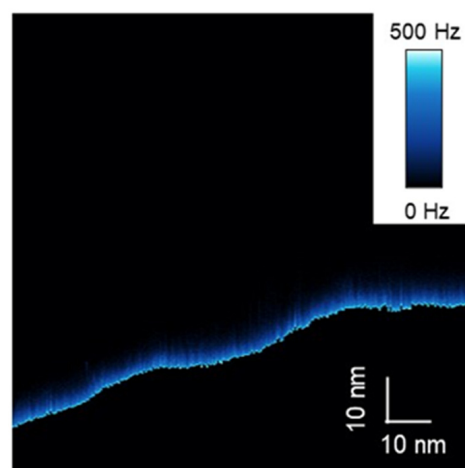


**Figure 11.** FM-AFM z-scan image on the HUVEC/PBS interface.

#### 4. Conclusions

In conclusion, the comparison study of HUVEC–substrate and HUVEC–HUVEC adhesion strength revealed the mechanism of HUVECs monolayer formation on PMEA-coated substrates. HUVECs attachment, proliferation, and migration indicated the blood compatibility of PMEA as a coating material. HUVECs migration from bare PET to the PMEA-coated side is a sign of cell migration from the native blood vessel to the artificial graft. In addition, the HUVECs monolayers effectively suppressed platelet adhesion. Finally, the FM-AFM observation of the hydration layer of HUVECs may be attributed to the presence of the glycocalyx layer. A healthy glycocalyx contributes to the antithrombogenic property of the PMEA-coated surface. Based on our results, a confluent monolayer of HUVECs can prevent platelet adsorption. Therefore, the PMEA coating can mimic the native blood vessel and can be used as a construction material for the development of ASDBs for the antithrombogenic and confluent monolayer formation of ECs.

**Supplementary Materials:** The following supporting information can be downloaded at: <https://www.mdpi.com/article/10.3390/coatings12060869/s1>. Figure S1: Images of FM-AFM z—x scan on (left) PMEA/PBS and (right) PMPC/PBS interface.

**Author Contributions:** Conceptualization: D.M. and M.T.; methodology: M.A.H., D.M., T.A. and M.T.; formal analysis: M.A.H.; investigation: M.A.H. and D.M.; data curation: M.A.H.; writing—original draft preparation: M.A.H.; writing—review and editing: D.M., T.A. and M.T.; supervision: D.M., T.A. and M.T.; project administration: M.T.; funding acquisition: M.T. All authors have read and agreed to the published version of the manuscript.

**Funding:** This study was funded by the Japan Society for the Promotion of Science (JSPS) (19H05720) from the Ministry of Education, Culture, Sports, Science and Technology of Japan.

**Institutional Review Board Statement:** Not applicable.

**Informed Consent Statement:** Not applicable.

**Data Availability Statement:** The authors confirm that the data supporting the findings of this study are available within the article.

**Acknowledgments:** We thank the Government of Japan (MEXT) for providing a scholarship for conducting this study and research at Kyushu University.

**Conflicts of Interest:** The authors declare no conflict of interest.

#### References

1. WHO. Cardiovascular Diseases (CVDs)—World Health Organization. 2017. Available online: [www.who.int/News-Room/Fact-Sheets/Detail/Cardiovascular-Diseases-\(Cvds\)](http://www.who.int/News-Room/Fact-Sheets/Detail/Cardiovascular-Diseases-(Cvds)) (accessed on 1 May 2022).
2. Smith, S.C.; Collins, A.; Ferrari, R.; Holmes, D.R.; Logstrup, S.; McGhie, D.V.; Ralston, J.; Sacco, R.L.; Stam, H.; Taubert, K.; et al. Our time: A call to save preventable death from cardiovascular disease (heart disease and stroke). *Glob. Heart* **2012**, *7*, 297–305. [CrossRef] [PubMed]
3. Mallis, P.; Kostakis, A.; Stavropoulos-Giokas, C.; Michalopoulos, E. Future perspectives in small-diameter vascular graft engineering. *Bioengineering* **2020**, *7*, 160. [CrossRef] [PubMed]
4. Xue, L.; Greisler, H.P. Biomaterials in the development and future of vascular grafts. *J. Vasc. Surg.* **2003**, *37*, 472–480. [CrossRef]
5. Eckmann, D.M.; Tsai, I.Y.; Tomczyk, N.; Weisel, J.W.; Composto, R.J. Hyaluronan and dextran modified tubes resist cellular activation with blood contact. *Colloids Surf. B Biointerfaces* **2013**, *108*, 44–51. [CrossRef]
6. PThalla, K.; Fadlallah, H.; Liberelle, B.; Lequoy, P.; de Crescenzo, G.; Merhi, Y.; Lerouge, S. Chondroitin sulfate coatings display low platelet but high endothelial cell adhesive properties favorable for vascular implants. *Biomacromolecules* **2014**, *15*, 2512–2520. [CrossRef] [PubMed]
7. Gao, A.; Hang, R.; Li, W.; Zhang, W.; Li, P.; Wang, G.; Bai, L.; Yu, X.F.; Wang, H.; Tong, L.; et al. Linker-free covalent immobilization of heparin, SDF-1 $\alpha$ , and CD47 on PTFE surface for antithrombogenicity, endothelialization and anti-inflammation. *Biomaterials* **2017**, *140*, 201–211. [CrossRef] [PubMed]
8. Weidenbacher, L.; Müller, E.; Guex, A.G.; Zündel, M.; Schweizer, P.; Marina, V.; Adlhart, C.; Vejsadová, L.; Pauer, R.; Spiecker, E.; et al. In Vitro Endothelialization of Surface-Integrated Nanofiber Networks for Stretchable Blood Interfaces. *ACS Appl. Mater. Interfaces* **2019**, *11*, 5740–5751. [CrossRef]

9. Radke, D.; Jia, W.; Sharma, D.; Fena, K.; Wang, G.; Goldman, J.; Zhao, F. Tissue Engineering at the Blood-Contacting Surface: A Review of Challenges and Strategies in Vascular Graft Development. *Adv. Healthc. Mater.* **2018**, *7*, 1701461. [\[CrossRef\]](#)
10. Noy, J.-M.; Chen, F.; Akhter, D.T.; Houston, Z.H.; Fletcher, N.L.; Thurecht, K.J.; Stenzel, M.H. Direct Comparison of Poly(ethylene glycol) and Phosphorylcholine Drug-Loaded Nanoparticles In Vitro and In Vivo. *Biomacromolecules* **2020**, *21*, 2320–2333. [\[CrossRef\]](#)
11. Furuzono, T.; Ishihara, K.; Nakabayashi, N.; Tamada, Y. Chemical modification of silk fibroin with 2-methacryloyloxyethyl phosphorylcholine. II. Graft-polymerization onto fabric through 2-methacryloyloxyethyl isocyanate and interaction between fabric and platelets. *Biomaterials* **2000**, *21*, 327–333. [\[CrossRef\]](#)
12. Park, H.H.; Sun, K.; Seong, M.; Kang, M.; Park, S.; Hong, S.; Jung, H.; Jang, J.; Kim, J.; Jeong, H.E. Lipid-Hydrogel-Nanostructure Hybrids as Robust Biofilm-Resistant Polymeric Materials. *ACS Macro Lett.* **2019**, *8*, 64–69. [\[CrossRef\]](#) [\[PubMed\]](#)
13. Hoffmann, J.; Groll, J.; Heuts, J.; Rong, H.; Klee, D.; Ziemer, G.; Moeller, M.; Wendel, H.P. Blood cell and plasma protein repellent properties of Star-PEG-modified surfaces. *J. Biomater. Sci. Polym. Ed.* **2006**, *17*, 985–996. [\[CrossRef\]](#) [\[PubMed\]](#)
14. Zhang, M.; Desai, T.; Ferrari, M. Proteins and cells on PEG immobilized silicon surfaces. *Biomaterials* **1998**, *19*, 953–960. [\[CrossRef\]](#)
15. Ratner Buddy, D.J. Blood compatibility—A perspective. *J. Biomater. Sci. Polym. Ed.* **2000**, *11*, 1107–1119. [\[CrossRef\]](#)
16. Kidane, A.; Lantz, G.C.; Jo, S.; Park, K. Surface modification with PEO-containing triblock copolymer for improved biocompatibility: In vitro and ex vivo studies. *J. Biomater. Sci. Polym. Ed.* **1999**, *10*, 1089–1105. [\[CrossRef\]](#)
17. Stetsyshyn, Y.; Raczowska, J.; Harhay, K.; Gajos, K.; Melnyk, Y.; Dąbczyński, P.; Shevtsova, T.; Budkowski, A. Temperature-responsive and multi-responsive grafted polymer brushes with transitions based on critical solution temperature: Synthesis, properties, and applications. *Colloid Polym. Sci.* **2021**, *299*, 363–383. [\[CrossRef\]](#)
18. Liu, Q.; Urban, M.W. Stimulus-Responsive Macromolecules in Polymeric Coatings. *Polym. Rev.* **2022**, in press. [\[CrossRef\]](#)
19. Bordenave, L.; Fernandez, P.; Rémy-Zolghadri, M.; Villars, S.; Daculsi, R.; Midy, D. In vitro endothelialized ePTFE prostheses: Clinical update 20 years after the first realization. *Clin. Hemorheol. Microcirc.* **2005**, *33*, 227–234.
20. Deutsch, M.; Meinhart, J.; Fischlein, T.; Preiss, P.; Zilla, P. Clinical autologous in vitro endothelialization of infrainguinal ePTFE grafts in 100 patients: A 9-year experience. *Surgery* **1999**, *126*, 847–855. [\[CrossRef\]](#)
21. Feugier, P.; Black, R.A.; Hunt, J.A.; How, T.V. Attachment, morphology and adherence of human endothelial cells to vascular prosthesis materials under the action of shear stress. *Biomaterials* **2005**, *26*, 1457–1466. [\[CrossRef\]](#)
22. Tanaka, M.; Motomura, T.; Kawada, M.; Anzai, T.; Kasori, Y.; Shiroya, T.; Shimura, K.; Onishi, M.; Mochizuki, A. Blood compatible aspects of poly(2-methoxyethylacrylate) (PMEA)-relationship between protein adsorption and platelet adhesion on PMEA surface. *Biomaterials* **2000**, *21*, 1471–1481. [\[CrossRef\]](#)
23. Tanaka, M.; Mochizuki, A.; Ishii, N.; Motomura, T.; Hatakeyama, T. Study of blood compatibility with poly(2-methoxyethyl acrylate). Relationship between water structure and platelet compatibility in poly(2-methoxyethylacrylate-co-2-hydroxyethylmethacrylate). *Biomacromolecules* **2002**, *3*, 36–41. [\[CrossRef\]](#) [\[PubMed\]](#)
24. Hatakeyama, T.; Tanaka, M.; Hatakeyama, H. Thermal properties of freezing bound water restrained by polysaccharides. *J. Biomater. Sci. Polym. Ed.* **2010**, *21*, 1865–1875. [\[CrossRef\]](#) [\[PubMed\]](#)
25. Murakami, D.; Kobayashi, S.; Tanaka, M. Interfacial Structures and Fibrinogen Adsorption at Blood-Compatible Polymer/Water Interfaces. *ACS Biomater. Sci. Eng.* **2016**, *2*, 2122–2126. [\[CrossRef\]](#)
26. Kobayashi, S.; Wakui, M.; Iwata, Y.; Tanaka, M. Poly( $\omega$ -methoxyalkyl acrylate)s: Nonthrombogenic Polymer Family with Tunable Protein Adsorption. *Biomacromolecules* **2017**, *18*, 4214–4223. [\[CrossRef\]](#)
27. Hatakeyama, T.; Tanaka, M.; Hatakeyama, H. Studies on bound water restrained by poly(2-methacryloyloxyethyl phosphorylcholine): Comparison with polysaccharide-water systems. *Acta Biomater.* **2010**, *6*, 2077–2082. [\[CrossRef\]](#)
28. McGuigan, A.P.; Sefton, M.V. The influence of biomaterials on endothelial cell thrombogenicity. *Biomaterials* **2007**, *28*, 2547–2571. [\[CrossRef\]](#)
29. Kitakami, E.; Aoki, M.; Sato, C.; Ishihata, H.; Tanaka, M. Adhesion and proliferation of human periodontal ligament cells on poly(2-methoxyethyl acrylate). *BioMed Res. Int.* **2014**, *2014*, 102648. [\[CrossRef\]](#)
30. Fearon, I.M.; Gaça, M.D.; Nordskog, B.K. In vitro models for assessing the potential cardiovascular disease risk associated with cigarette smoking. *Toxicol In Vitro* **2013**, *27*, 513–522. [\[CrossRef\]](#)
31. Medina-Leyte, D.J.; Domínguez-Pérez, M.; Mercado, I.; Villarreal-Molina, M.T.; Jacobo-Albavera, L. Use of human umbilical vein endothelial cells (HUVEC) as a model to study cardiovascular disease: A review. *Appl. Sci.* **2020**, *10*, 938. [\[CrossRef\]](#)
32. Carmeliet, P.; Jain, R.K. Molecular mechanisms and clinical applications of angiogenesis. *Nature* **2011**, *473*, 298–307. [\[CrossRef\]](#) [\[PubMed\]](#)
33. Zhao, Z.; Sun, W.; Guo, Z.; Zhang, J.; Yu, H.; Liu, B. Mechanisms of lncRNA/microRNA interactions in angiogenesis. *Life Sci.* **2020**, *254*, 116900. [\[CrossRef\]](#) [\[PubMed\]](#)
34. Chen, Y.M.; Tanaka, M.; Gong, J.P.; Yasuda, K.; Yamamoto, S.; Shimomura, M.; Osada, Y. Platelet adhesion to human umbilical vein endothelial cells cultured on anionic hydrogel scaffolds. *Biomaterials* **2007**, *28*, 1752–1760. [\[CrossRef\]](#) [\[PubMed\]](#)
35. Mahmoud, M.; Cancel, L.; Tarbell, J.M. Matrix Stiffness Affects Glycocalyx Expression in Cultured Endothelial Cells. *Front. Cell Dev. Biol.* **2021**, *9*, 731666. [\[CrossRef\]](#) [\[PubMed\]](#)
36. Hoshiba, T.; Orui, T.; Endo, C.; Sato, K.; Yoshihiro, A.; Minagawa, Y.; Tanaka, M. Adhesion-based simple capture and recovery of circulating tumor cells using a blood-compatible and thermo-responsive polymer-coated substrate. *RSC Adv.* **2016**, *6*, 89103–89112. [\[CrossRef\]](#)

37. Nishida, K.; Anada, T.; Kobayashi, S.; Ueda, T.; Tanaka, M. Effect of bound water content on cell adhesion strength to water-insoluble polymers. *Acta Biomater.* **2021**, *134*, 313–324. [[CrossRef](#)]
38. Friedrichs, J.; Legate, K.R.; Schubert, R.; Bharadwaj, M.; Werner, C.; Müller, D.J.; Benoit, M. A practical guide to quantify cell adhesion using single-cell force spectroscopy. *Methods* **2013**, *60*, 169–178. [[CrossRef](#)]
39. Tanaka, M.; Motomura, T.; Kawada, M.; Anzai, T.; Kasori, Y.; Shimura, K.; Onishi, M.; Mochizuki, A.; Okahata, Y. A New Blood-Compatible Surface Prepared by Poly (2-methoxyethylacrylate) (PMEA) Coating-Protein Adsorption on PMEA Surface. *Jpn. J. Artif. Organs* **2000**, *29*, 209–216. [[CrossRef](#)]
40. Krüger-Genge, A.; Hauser, S.; Neffe, A.T.; Liu, Y.; Lendlein, A.; Pietzsch, J.; Jung, F. Response of Endothelial Cells to Gelatin-Based Hydrogels. *ACS Biomater. Sci. Eng.* **2021**, *7*, 527–540. [[CrossRef](#)]
41. Sato, C.; Aoki, M.; Tanaka, M. Blood-compatible poly(2-methoxyethyl acrylate) for the adhesion and proliferation of endothelial and smooth muscle cells. *Colloids Surf. B Biointerfaces* **2016**, *145*, 586–596. [[CrossRef](#)]
42. Kono, K.; Hiruma, H.; Kobayashi, S.; Sato, Y.; Tanaka, M.; Sawada, R.; Niimi, S. In vitro endothelialization test of biomaterials using immortalized endothelial cells. *PLoS ONE* **2016**, *11*, e0158289. [[CrossRef](#)] [[PubMed](#)]
43. Hozumi, K.; Otagiri, D.; Yamada, Y.; Sasaki, A.; Fujimori, C.; Wakai, Y.; Uchida, T.; Katagiri, F.; Kikkawa, Y.; Nomizu, M. Cell surface receptor-specific scaffold requirements for adhesion to laminin-derived peptide-chitosan membranes. *Biomaterials* **2010**, *31*, 3237–3243. [[CrossRef](#)] [[PubMed](#)]
44. Hersel, U.; Dahmen, C.; Kessler, H. RGD modified polymers: Biomaterials for stimulated cell adhesion and beyond. *Biomaterials* **2003**, *24*, 4385–4415. [[CrossRef](#)]
45. Hoshiba, T.; Yoshihiro, A.; Tanaka, M. Evaluation of initial cell adhesion on poly (2-methoxyethyl acrylate) (PMEA) analogous polymers. *J. Biomater. Sci. Polym. Ed.* **2017**, *28*, 986–999. [[CrossRef](#)] [[PubMed](#)]
46. Sancho, A.; Vandersmissen, I.; Craps, S.; Lutun, A.; Groll, J. A new strategy to measure intercellular adhesion forces in mature cell-cell contacts. *Sci. Rep.* **2017**, *7*, 46152. [[CrossRef](#)] [[PubMed](#)]
47. Zeng, Y.; Zhang, X.F.; Fu, B.M.; Tarbell, J.M. The role of endothelial surface glycocalyx in mechanosensing and transduction. In *Advances in Experimental Medicine and Biology*; Springer: New York, NY, USA, 2018; pp. 1–27. [[CrossRef](#)]
48. Félétou, M. The Endothelium, Part I: Multiple Functions of the Endothelial Cells—Focus on Endothelium-Derived Vasoactive Mediators. In *Colloquium Series on Integrated Systems Physiology: From Molecule to Function*; Morgan & Claypool Life Sciences: San Rafael, CA, USA, 2011; Volume 3, pp. 1–306. [[CrossRef](#)]
49. Gori, T.; von Henning, U.; Muxel, S.; Schaefer, S.; Fasola, F.; Vosseler, M.; Schnorbus, B.; Binder, H.; Parker, J.D.; Münzel, T. Both flow-mediated dilation and constriction are associated with changes in blood flow and shear stress: Two complementary perspectives on endothelial function. *Clin. Hemorheol. Microcirc.* **2016**, *64*, 255–266. [[CrossRef](#)]
50. Murakami, D.; Kitahara, Y.; Kobayashi, S.; Tanaka, M. Thermosensitive Polymer Biocompatibility Based on Interfacial Structure at Biointerface. *ACS Biomater. Sci. Eng.* **2018**, *4*, 1591–1597. [[CrossRef](#)]
51. Murakami, D.; Nishimura, S.; Tanaka, Y.; Tanaka, M. Observing the repulsion layers on blood-compatible polymer-grafted interfaces by frequency modulation atomic force microscopy. *Mater. Sci. Eng C* **2022**, *133*, 112596. [[CrossRef](#)]